



Structural and theoretical studies of [6-bromo-1-(4-fluorophenylmethyl)-4(1*H*)-quinolinon-3-yl]-4-hydroxy-2-oxo-3-butenic acid as HIV-1 integrase inhibitor

Pierre Vandurm^{a,*,†}, Christine Cauvin^{a,†}, Allan Guiguen^{b,†}, Benoît Georges^c, Kiet Le Van^c, Valérie Martinelli^b, Christelle Cardona^b, Gladys Mbemba^d, Jean-François Mouscadet^d, László Hevesi^{c,‡}, Carine Van Lint^{b,‡}, Johan Wouters^{a,‡}

^aLaboratoire de Chimie Biologique Structurale, Facultés Universitaires Notre-Dame de la Paix (FUNDP), B-5000 Namur, Belgium

^bLaboratoire de Virologie Moléculaire, Institut de Biologie et de Médecine Moléculaires, Université Libre de Bruxelles (ULB), B-6041 Gosselies, Belgium

^cLaboratoire de Chimie des Matériaux Organiques, Facultés Universitaires Notre-Dame de la Paix (FUNDP), B-5000 Namur, Belgium

^dLaboratoire de Biotechnologies et de Pharmacologie Génétique Appliquée, CNRS, Ecole Normale Supérieure de Cachan (ENS), F-94235 Cachan, France

ARTICLE INFO

Article history:

Received 6 May 2009

Revised 8 June 2009

Accepted 11 June 2009

Available online 14 June 2009

Keywords:

HIV-1

Integrase inhibitors

Quinolinone

β-Diketo

ABSTRACT

Ethyl [6-bromo-1-(4-fluorophenylmethyl)-4(1*H*)-quinolinon-3-yl]-4-hydroxy-2-oxo-3-butenate **1** and [6-bromo-1-(4-fluorophenylmethyl)-4(1*H*)-quinolinon-3-yl]-4-hydroxy-2-oxo-3-butenic acid **2** were synthesized as potential HIV-1 integrase inhibitors and evaluated for their enzymatic and antiviral activity, acidic compound **2** being more potent than ester compound **1**. X-ray diffraction analyses and theoretical calculations show that the diketoacid chain of compound **2** is preferentially coplanar with the quinolinone ring (dihedral angle of 0–30°). Docking studies suggest binding modes in agreement with structure–activity relationships.

© 2009 Elsevier Ltd. All rights reserved.

HIV integrase (IN) is currently recognized as an attractive target against AIDS. It catalyzes the integration of reverse transcribed viral DNA into host cell DNA through a two-step, metal-dependent process.¹ Step one, known as 3' processing (3'-P), effects cleavage of two nucleotides from the two 3' ends of double stranded viral DNA. The second step, strand transfer (ST), integrates the viral DNA into the host cell DNA through phosphodiester transesterification reactions. Integrase is an especially attractive target for HIV therapy because the enzyme is needed for viral infectivity and there are no known host cell counterparts.²

In the past several years, compounds with diverse structural features have been reported as IN inhibitors.³ Among those IN inhibitors, compounds containing the β-diketoacid (DKA) moiety were extensively studied. S1360⁴ (Fig. 1) has entered clinical trials but its development was stopped due to pharmacokinetic problems. More recently, other promising DKA-based derivatives have reached advanced clinical development: raltegravir (Fig. 1) is the

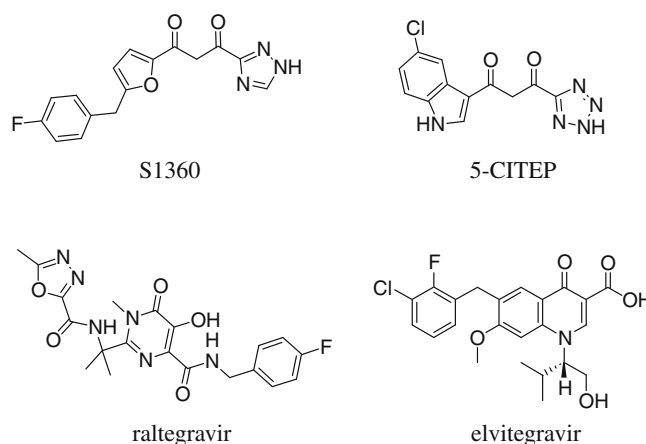


Figure 1. Structures of DKA-based integrase inhibitors.

* Corresponding author. Tel.: +32 81724569; fax: +32 81725440.

E-mail address: pierre.vandurm@fundp.ac.be (P. Vandurm).

† These authors contributed equally to this work.

‡ These authors co-directed the present study (e-mail address: laszlo.hevesi@fundp.ac.be, cvlint@ulb.ac.be, johan.wouters@fundp.ac.be). CVL is Directeur de Recherches of the Belgian 'Fonds de la Recherche Scientifique-FNRS' (FRS-FNRS).

first FDA approved IN inhibitor (since October 2007) whereas elvitegravir (Fig. 1) is presently in phase III clinical trials.⁵ All these IN inhibitors contain a chelating moiety involved in sequestration of divalent metal cofactors at the enzyme catalytic site.⁶ A DKA

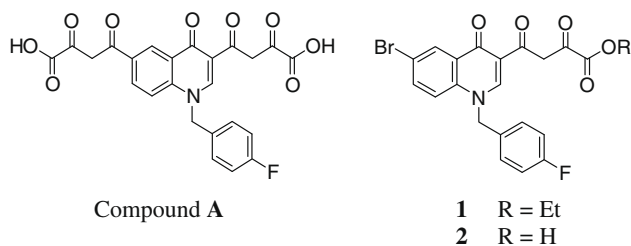


Figure 2. Structures of quinolinone reference compound **A**⁸ and 6-bromine analogues **1** and **2**.

compound, the 5-CITEP (Fig. 1), was cocrystallized with the catalytic core domain of the enzyme.⁷ X-ray crystal structure of the complex showed that 5-CITEP binds in the middle of the active site of the enzyme, lying between the three catalytic acidic residues, D64, D116 and E152, in the vicinity of the active site metal ion.

Recently, some DKA derivatives containing the quinolinone scaffold have been reported.^{8,9} Among these, compound **A** (Fig. 2) displays a good anti-integrase activity for both 3'-P and ST (IC₅₀ (3'-P) = 0.44 μM; IC₅₀ (ST) = 0.017 μM). Based on this quinolinone series, we have synthesized 6-bromide analogues with an ester (compound **1**, Fig. 2) or an acidic group (compound **2**, Fig. 2) on the diketo moiety. In this Letter, we disclose the synthesis, anti-integrase and antiviral data of these compounds. We discuss also on conformation and potential binding modes of compound **2** from crystallographic analyses and modelling studies.

Synthesis of compounds **1** and **2** was achieved by adapting a method previously reported by Di Santo et al.⁸ (see Supplementary data). The requisite intermediate 3-acetyl-6-bromo-4(1*H*)-quinolinone **5** was obtained by reaction of commercially available 4-bromoaniline with ethylethoxymethylacetate and subsequent thermic cyclization in diphenyl ether. **5** was then N-alkylated with 4-fluorobenzyl bromide in alkaline medium to give compound **6** which then underwent Claisen condensation with diethyl oxalate in the presence of sodium ethoxide to afford diketo ester **1**. Alkaline hydrolysis of **1** led to **2**. Compounds **1** and **2** obtained, respectively, in 74% and 93%, were fully characterized by IR, ¹H NMR, ¹³C NMR and MS.

Both compounds were evaluated for their anti-integrase,¹⁰ antiviral activity¹¹ and cytotoxicity (Table 1). Compound **2** exhibited better inhibitory activity against IN than compound **1**.

The antiviral activities are correlated with the anti-integrase activities, compound **2** displaying an EC₅₀ of 4.0 μM versus 17 μM for compound **1** (TZM-bl cells). These data are in agreement with previous results showing higher potency for DKA compounds.¹² Concerning anti-integrase activity, both compounds showed a much better selectivity for the strand transfer versus 3'-processing reaction. Interestingly, both derivatives have low cytotoxicity (CC₅₀ > 1 mM) against HIV-1 infected TZM-bl cells.

In order to predict the potential binding mode of compound **2** in the enzyme, we first performed conformational analyses on the

Table 1

IN inhibition data (IC₅₀), antiviral activity (EC₅₀, TZM-bl cells) and cytotoxicity (CC₅₀) of compounds **1** and **2**

Compound	IC ₅₀ (3'-P) ^a (μM)	IC ₅₀ (ST) ^b (μM)	EC ₅₀ ^c (μM)	CC ₅₀ ^d (μM)	SI ^e
1	78	0.12	17	>1000	>59
2	1.6	0.03	4.0	>1000	>250

^a Inhibitory concentration 50% for 3'-processing.¹⁰

^b Inhibitory concentration 50% for strand transfer.¹⁰

^c Effective concentration 50% (TZM-bl cells).¹¹

^d Cytotoxic concentration 50% (TZM-bl cells).

^e Selectivity index CC₅₀/EC₅₀.

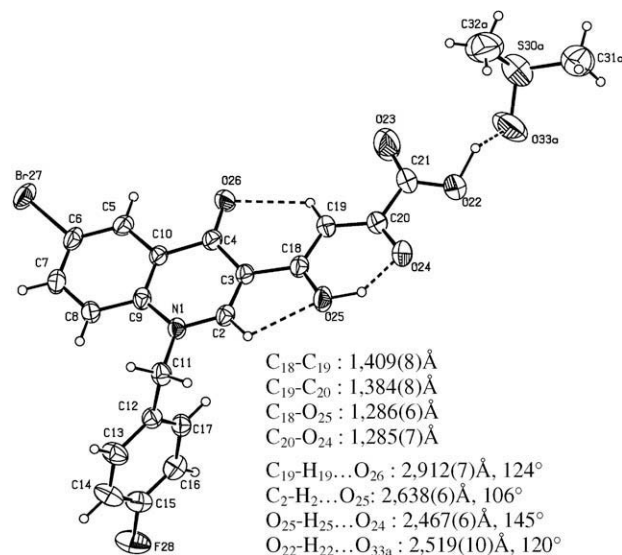


Figure 3. Crystal structure of compound **2** (cocrystallized with DMSO) showing the atom-numbering and hydrogen-bonding scheme. Displacement ellipsoids are drawn at the 30% level.¹⁹ Selected distances (Å) and angles (°) are also reported for the keto–enol moiety.

uncomplexed derivative using X-ray diffraction (XRD) and theoretical calculations.

Crystal structure of **2** is shown in Figure 3. This compound cocrystallized with DMSO, both molecules being linked by hydrogen bonds between carboxylic acid group and DMSO oxygen O_{33a}. The DKA chain and the quinolinone ring of compound **2** are nearly coplanar with dihedral angle C₄–C₃–C₁₈–O₂₅ of 177°. The orientation of the diketo moiety with respect to the quinolinone ring is governed by intramolecular C₂–H₂...O₂₅ and C₁₉–H₁₉...O₂₆ hydrogen bonds. In this solid-state structure, the equilibrium between β-diketo and keto enol forms is displaced in favour of the keto–enol isomer, the hydrogens on C₁₉ and O₂₅ being clearly identified by Fourier difference. However, it is difficult to discriminate between the two potential keto–enol tautomers. Indeed, H₂₅ is involved in a strong hydrogen bond with O₂₄ and the O₂₅–H₂₅ distance (1.06 Å) is greater than commonly observed for O–H bonds (0.82 Å). Furthermore, both carbonyl (C₁₈–O₂₅ and C₂₀–O₂₄) and carbon–carbon (C₁₈–C₁₉ and C₁₉–C₂₀) bond distances are similar and intermediate between standard single and double bonds, indicative of strong electronic delocalization within this keto–enol moiety.

In order to further explore the preferential relative orientation of the DKA chain and quinolinone ring, we performed a conformational scan on the C₁₉–C₁₈–C₃–C₂ torsion angle (T1) using a truncated molecule (without bromine atom and *p*-F-phenyl moiety) (Fig. 4). The scan was realized considering both potential keto–enol tautomers (a and b, Fig. 4).

The quantum chemistry calculations were carried out at the pbe1pbe level of theory with 6-31G** basis set using GAUSSIAN 03 software.¹³ At each step of the scan (from 0° to 180° with an increment of 15°), the conformation was optimized and the energy evaluated. Figure 4 depicts ΔE (energy difference between considered conformation and global energy minimum) as a function of torsion angle T1. Both tautomers present a similar energetic profile (ΔE between tautomers less than 1 kcal/mol), the most stable conformation being observed for a torsion angle of 180°. Interestingly, this conformer corresponds to the crystal structure of compound **2**, showing correlations between theoretical and experimental results. Another local minimum is observed for a T1 value of 30° (ΔE of 7–8 kcal/mol). The conformer with T1 of 0° is more ener-

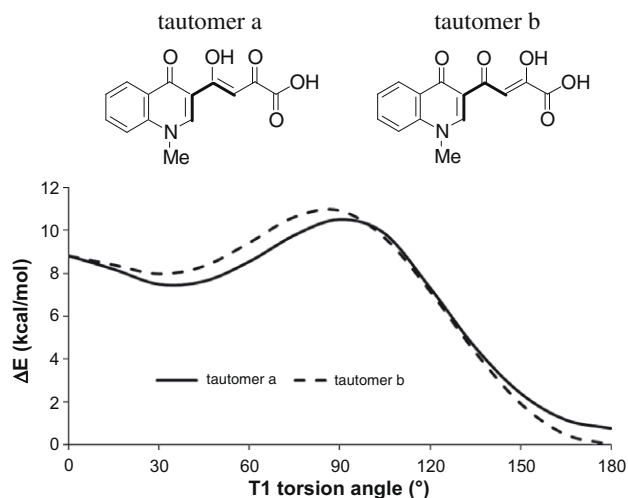


Figure 4. Conformational results for torsion angle T1 (pbe1pbe/6-31G^{**}). Relative energies (ΔE) are calculated using the global minimum (T1 = 180°, tautomer b) as reference.

getic due to steric hindrance. As expected, the conformation with T1 of 90° presents the highest energy due to full lack of conjugation. Based on these theoretical results, conformers with T1 of

30° and 180° were considered for further modelling studies of compound **2**.

In an attempt to predict the binding mode of compound **2** into the integrase catalytic core domain, docking studies¹⁴ were performed using the X-ray structure of the protein (PDB code: 1BL3, subunit C).¹⁵ Figure 5a depicts the catalytic site located at the surface of the enzyme and composed of three main pockets and Mg²⁺ metal ion. In the first hydrophilic pocket, the two conserved residues D64 and D116 chelate the Mg²⁺ cofactor essential for the catalytic activity of the enzyme. The second pocket is mainly constituted by hydrophilic residues known to be critical for viral DNA ends binding (K156, K159)¹⁶ or to be associated with resistance to strand transfer inhibitors (N155).¹⁷ The third hydrophobic pocket including P142, Y143, N144, P145, Q146, S147, Q148, G149 and Q62 residues, forms a catalytic loop involved in the binding of the host DNA and viral DNA ends.¹⁸

Docking studies of compound **2** were performed on both tautomers using the most stable conformations identified by theoretical calculations (T1 of 30° and 180°).

Best binding modes were obtained for compound with b keto-enol tautomeric form. Two predominant poses with DKA moiety close to Mg²⁺ metal ion were identified (Fig. 5b). In the first one (Fig. 5b left, T1 equal to 30°), the Mg²⁺ is chelated in a bidentate manner by the two oxygens of the diketo moiety (with D64 and D116). The *p*-F-benzyl group points toward the catalytic loop and

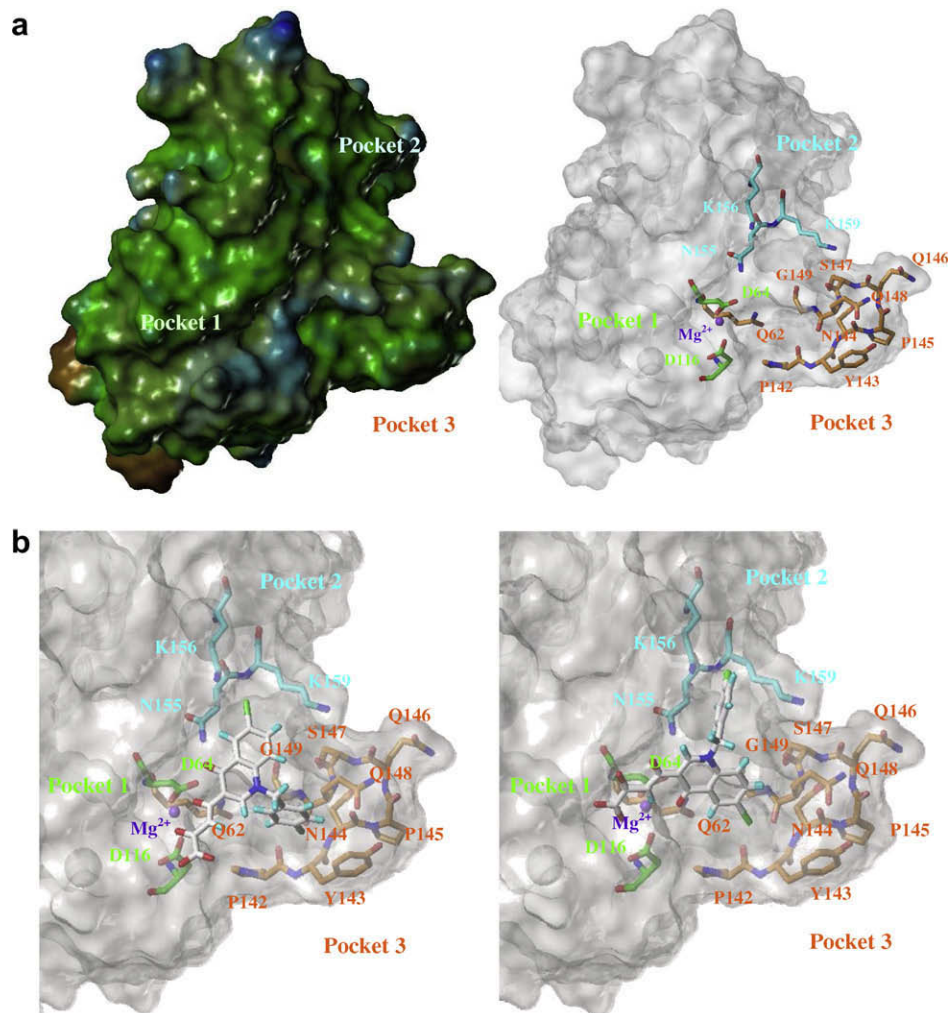


Figure 5. (a) Catalytic domain of integrase¹⁵ (pdb code:1BL3) with main residues and Mg²⁺ metal ion (purple). Pockets are coloured according hydrophobicity of residues (from blue to brown). This figure was prepared using the MOLCAD module of SYBYL8.0 program.^{14b} (b) Docking results of compound **2** into HIV-1 integrase active site (left, T1 = 30°; right, T1 = 180°).

the bromine atom inserts between K156 and K159 residues. The quinolinone ring is close to the N155 side chain. In the second binding mode depicted in Figure 5b right, the Mg^{2+} metal ion is chelated in a bidentate manner by the quinolinone carbonyl oxygen and by the carboxylate group. The bromine atom is oriented towards the catalytic loop and the *p*-F-benzyl moiety is located between K156 and K159. Both binding modes highlight the importance of the DKA moiety for the chelation of the Mg^{2+} and particularly the carboxylate group which could explain the stronger inhibitory potency of acidic compound **2** compared to ester compound **1**. At this stage, it is difficult to discriminate between the two proposed binding modes and one can not exclude other potential ones. Indeed, docking studies show some limitations such as the use of a rigid protein (and metal ion cofactor) and a scoring function which does not take correctly into account the energetic contributions issued from metal ion chelation and other weak interactions such as hydrogen bonds and van der Waals forces. Furthermore, the presence of viral DNA and the existence of a second Mg^{2+} in the catalytic pocket can be also considered as recently suggested.²⁰ The obtention of crystal structure of enzyme/DNA/inhibitor complexes should help to clarify the inhibition mechanism.

Nevertheless, these modelling studies show the relevance of synthesizing compounds able to simultaneously chelate metal ion (pocket 1) and fill the two other depicted cavities (pockets 2 and 3). Within this context, bromine atom could be replaced by various substituents depending on the binding mode considered. In the first binding mode (Fig. 5b left), bromine atom could be substituted by anionic groups able to form electrostatic interactions with K156 and K159 residues. In the second binding mode (Fig. 5b right), the bromine could be replaced by big hydrophobic moieties filling pocket 3. These pharmacomodulations should increase the inhibitory potency of our series of derivatives. Furthermore, resulting structure–activity relationships should help to discriminate between binding modes.

Acknowledgments

This research was supported by grants from the DGTRE (Direction générale des Technologies, de la Recherche et de l'Énergie, Région Wallonne) (Programs WALEO). P. Vandurm thanks F.R.I.A for financial support. We also thank the mass spectrometry laboratory of Catholic University of Leuven (Raoul Rozenberg and Alexander Spote).

Supplementary data

Chemistry: synthetic pathway and compounds spectroscopic data; biology: protocols for in vitro experiments, antiviral activities and cytotoxicity measurements; structural and modelling studies: crystal data and docking parameters. CCDC 730039 contains the supplementary crystallographic data for this paper. These data can be obtained free of charge from The Cambridge Crystallographic Data Centre via www.ccdc.cam.ac.uk/data_request/cif.

Supplementary data associated with this article can be found, in the online version, at [doi:10.1016/j.bmcl.2009.06.044](https://doi.org/10.1016/j.bmcl.2009.06.044).

References and notes

- (a) Engelman, A.; Mizuuchi, K.; Craigie, R. *Cell* **1991**, *67*, 1211; (b) Chiu, T. K.; Davies, D. R. *Curr. Top. Med. Chem.* **2004**, *4*, 965; (c) Delelis, O.; Carayon, K.; Sa, A.; Deprez, E.; Mouscadet, J.-F. *Retrovirology* **2008**, *5*, 114.
- (a) LaFemina, R. L.; Schneider, C. L.; Robbins, H. L.; Callahan, P. L.; LeGrow, K.; Roth, E.; Schleif, W. A.; Emini, E. A. *J. Virol.* **1992**, *66*, 7414; (b) Debyser, Z.; Cherepanov, P.; Van Maele, B.; De Clercq, E.; Witvrouw, M. *Antiviral Chem. Chemother.* **2002**, *13*, 1.
- (a) Cotellet, P. *Recent Pat. Anti-Infect. Drug Discovery* **2006**, *1*, 1; (b) Dubey, S.; Satyanarayana, Y. D.; Lavania, H. *Eur. J. Med. Chem.* **2007**, *42*, 1159; (c) Makhija, M. T. *Curr. Med. Chem.* **2006**, *13*, 2429; (d) Serrao, E.; Odde, S.; Ramkumar, K.; Neamati, N. *Retrovirology* **2009**, *6*, 25.
- Billich, A. *Curr. Opin. Invest. Drugs* **2003**, *4*, 206.
- (a) Summa, V.; Petrocchi, A.; Bonelli, F.; Crescenzi, B.; Donghi, M.; Ferrara, M.; Fiore, F.; Gardelli, C.; Gonzalez Paz, O.; Hazuda, D. J.; Jones, P.; Kinzel, O.; Laufer, R.; Monteagudo, E.; Muraglia, E.; Nizi, E.; Orvieto, F.; Pace, P.; Pescatore, G.; Scarpelli, R.; Stillmock, K.; Witmer, M. V.; Rowley, M. *J. Med. Chem.* **2008**, *51*, 5843; (b) Sato, M.; Motomura, T.; Aramaki, H.; Matsuda, T.; Yamashita, M.; Ito, Y.; Kawakami, H.; Matsuzaki, Y.; Watanabe, W.; Yamataka, K.; Ikeda, S.; Kodama, E.; Matsuoka, M.; Shinkai, H. *J. Med. Chem.* **2006**, *49*, 1506; (c) Hazuda, D.; Iwamoto, M.; Wenning, L. *Annu. Rev. Pharmacol. Toxicol.* **2009**, *49*, 377.
- (a) Hazuda, D. J.; Felock, P.; Witmer, M.; Wolfe, A.; Stillmock, K.; Grobler, J. A.; Espeseth, A.; Gabryelski, L.; Schleif, W.; Blau, C.; Miller, M. D. *Science* **2000**, *287*, 646; (b) Grobler, J. A.; Stillmock, K.; Hu, B.; Witmer, M.; Felock, P.; Espeseth, A. S.; Wolfe, A.; Egbertson, M.; Bourgeois, M.; Melamed, J.; Wai, J. S.; Young, S.; Vacca, J.; Hazuda, D. J. *Proc. Natl. Acad. Sci. U.S.A.* **2002**, *99*, 6661; (c) Pommier, Y.; Johnson, A. A.; Marchand, C. *Nat. Rev. Drug Discovery* **2005**, *4*, 236; (d) Bacchi, A.; Biemmi, M.; Carcelli, M.; Carta, F.; Compari, C.; Fiscaro, E.; Rogolino, D.; Sechi, M.; Sippel, M.; Sottriffer, C. A.; Sanchez, T. W.; Neamati, N. *J. Med. Chem.* **2008**, *51*, 7253.
- Goldgur, Y.; Craigie, R.; Cohen, G.; Fujiwara, T.; Yoshinaga, T.; Fujishita, T.; Sugimoto, H.; Endo, T.; Murai, H.; Davies, D. R. *Proc. Natl. Acad. Sci. U.S.A.* **1999**, *96*, 13040.
- Di Santo, R.; Costi, R.; Roux, A.; Artico, M.; Lavecchia, A.; Marinelli, L.; Novellino, E.; Palmisano, L.; Andreotti, M.; Amici, R.; Galluzzo, C. M.; Nencioni, L.; Palamara, A. T.; Pommier, Y.; Marchand, C. *J. Med. Chem.* **2006**, *49*, 1939.
- Di Santo, R.; Costi, R.; Roux, A.; Miele, G.; Crucitti, G. C.; Iacovo, A.; Rosi, F.; Lavecchia, A.; Marinelli, L.; Di Giovanni, C.; Novellino, E.; Palmisano, L.; Andreotti, M.; Amici, R.; Galluzzo, C. M.; Nencioni, L.; Palamara, A. T.; Pommier, Y.; Marchand, C. *J. Med. Chem.* **2008**, *51*, 4744.
- Leh, H.; Brodin, P.; Bischerour, J.; Deprez, E.; Tauc, P.; Brochon, J.-C.; LeCam, E.; Coulaud, D.; Auclair, C.; Mouscadet, J.-F. *Biochemistry* **2000**, *39*, 9285.
- Wei, X.; Decker, J. M.; Liu, H.; Zhang, Z.; Arani, R. B.; Kilby, J. M.; Saag, M. S.; Wu, X.; Shaw, G. M.; Kappes, J. C. *Antimicrob. Agents Chemother.* **2002**, *46*, 1896.
- (a) Pais, G. C. G.; Zhang, X.; Marchand, C.; Neamati, N.; Cowansage, K.; Svarovskaia, E. S.; Pathak, V. K.; Tang, Y.; Nicklaus, M.; Pommier, Y.; Burke, T. R. *J. Med. Chem.* **2002**, *45*, 3184; (b) Sechi, M.; Derudas, M.; Dallochio, R.; Dessi, A.; Bacchi, A.; Sanna, L.; Carta, F.; Palomba, M.; Ragab, O.; Chan, C.; Shoemaker, R.; Sei, S.; Dayam, R.; Neamati, N. *J. Med. Chem.* **2004**, *47*, 5298; (c) Patil, S.; Kamath, S.; Sanchez, T.; Neamati, N.; Schinazi, R. F.; Buolamwini, J. K. *Bioorg. Med. Chem.* **2007**, *15*, 1212.
- Frisch, M. J.; Trucks, G. W.; Schlegel, H. B.; Scuseria, G. E.; Robb, M. A.; Cheeseman, J. R.; Montgomery, Jr., J. A.; Vreven, T.; Kudin, K. N.; Burant, J. C.; et al. *GAUSSIAN 03*, Gaussian, Wallingford CT, 2004.
- (a) Jones, G.; Willett, P.; Glen, R. C.; Leach, A. R.; Taylor, R. *J. Mol. Biol.* **1997**, *267*, 727; (b) SYBYL 8.0, Tripos International, 1699 South Hanley Rd., St. Louis, Missouri 63144, USA.
- Maignan, S.; Guilloteau, J. P.; Zhou-Liu, Q.; Clement-Mella, C.; Mikol, V. *J. Mol. Biol.* **1998**, *282*, 359.
- Jenkins, T. M.; Esposito, D.; Engelman, A.; Craigie, R. *EMBO J.* **1997**, *16*, 6849.
- Alves, C. N.; Marti, S.; Castillo, R.; Andres, J.; Moliner, V.; Tunon, I.; Silla, E. *Biophys. J.* **2008**, *94*, 2443.
- Wielens, J.; Crosby, I. T.; Chalmers, D. K. *J. Comput. Aided Mol. Des.* **2005**, *19*, 301.
- Spek, A. L. 'PLATON: A Multipurpose Crystallographic Tool', 2001, University of Utrecht; Utrecht, The Netherlands.
- Ferro, S.; De Luca, L.; Barreca, M. L.; Iraci, N.; De Grazia, S.; Christ, F.; Witvrouw, M.; Debyser, Z.; Chimiri, A. *J. Med. Chem.* **2009**, *52*, 569.